Z. Phys. C – Particles and Fields 34, 103–115 (1987)

Zeitschrift für Physik C Particles and Fields

Exclusive Non-Leptonic Decays of D-, D_s- and B-Mesons

M. Bauer[1], B. Stech[1], M. Wirbel[2]

[1] Institut für Theoretische Physik der Universität, D-6900 Heidelberg, Federal Republic of Germany
[2] Institut für Theoretische Physik der Universität, D-4600 Dortmund, Federal Republic of Germany

Received 17 November 1986

Abstract. Recent experimental results on D-, D_s- and B-decays are interpreted on the basis of the valence quark model. For nonleptonic decays generally good results are obtained using factorization with little direct annihilation. Final state interaction causes corrections, however: small bare amplitudes can be fed by stronger amplitudes through channel mixing. This effect can simulate or enhance weak annihilation processes in particular if high lying resonances contribute. A comparison of $D^0 \to \bar{K}^0 \phi$ with $D_s \to \rho\pi$ decays will clarify this issue. The effective QCD coefficients obtained in the analysis are discussed and used to estimate the contribution of two-body decays to the total widths. The result reflects already the lifetime differences between D^0 and D^+ mesons. Predictions for numerous B-decay branching ratios allow for further tests and for a determination of so far unknown decay constants. A first bound on $|V_{ub}|$ from nonleptonic decays is found from the experimental limit on $\bar{B}^0 \to \pi^+\pi^-$.

1. Introduction

Historically, weak decays have always been an extraordinarily rich source of information about form and symmetry of the basic interactions as well as about the structure of the constituents of matter. This is still the case today. Weak decays are essential for testing the standard model and determining their fundamental quark mixing parameters. They also provide important information on the quark and gluon composition of hadrons not yet predictable from Quantum-Chromo-Dynamics.

Thanks to the efforts of the ARGUS, CLEO, DELCO, MARK II and especially MARK III collaborations a wealth of important data on D-, D_s- and B-decays is now available. The measured general form of the *semileptonic* D- and B-decay spectra [1] is in accord with the theoretical expectation from the V-A theory [2]. The theoretical description of semileptonic decays now concentrates on exclusive channels [3–5]. Thereby one avoids the uncertainties connected with quark masses, quark phase space and various confinement effects inherent in a pure quark decay picture. At least the high energy part of the lepton spectra is strongly influenced by exclusive channels. Their contribution is therefore essential for a determination of the fundamental ratio $|V_{ub}/V_{cb}|$ of Kobayashi-Maskawa matrix elements [3, 5]. In an exclusive treatment the decay widths are given in terms of measurable physical hadron matrix elements of the weak currents. Unfortunately, little is known about the structure of mesons consisting of a heavy and a light quark. In [3] we used relativistic oscillator wave functions at infinite momentum to estimate matrix elements of currents and found good agreement with the available data. More precise tests and a determination of the formfactor dependence on momentum transfer are needed, however.

In the present paper we turn to exclusive *nonleptonic* decays [6, 7] where again the matrix elements of currents enter in an essential way. In a first analysis [8] of the MARK III data [9] it was found that the pattern of energetic two-body decays follows qualitatively what one expects from a factorization approach. In the following we will present an updated and extended description of exclusive nonleptonic decays of heavy flavours where in addition to factorization also channel mixing and weak annihilation are considered. We will not discuss the problem of $D-\bar{D}$ and $B-\bar{B}$ mixing and CP violation in D- and B-decays (where we refer the reader to the literature [10]).

We start with a review of the various ways in which the flavour quantum numbers are changed and transmitted from the decaying meson to two final hadrons. Unfortunately amplitudes with identical flavour flow still depend on the specific initial and final meson due to different particle spins, quark masses and nonperturbative effects even though QCD forces are flavour independent. As a first step the factorization assumption will be used in Sect. 3. In this approximation the amplitudes are products of current matrix elements which can be calculated using the results of [3]. An extensive list of two-body decay amplitudes of D-, D_s- and B-mesons obtained in this way will be given in the appendix. In Sect. 4 we will discuss the effects of final state interaction for D-decays. An isospin analysis of the experimental data gives rise to substantial modifications for various decay channels. Since the D-meson lies in a resonance region rescattering of the two final mesons may be important. In particular, amplitudes which are small in the factorization approach may be fed from stronger channels by channel mixing. Weak annihilation, its enhancement by resonance scattering and its relation to channel mixing will be discussed in Sect. 5. In Sect. 6 we will present our results for exclusive nonleptonic D- and D_s-meson decays and make predictions for many two-body B-meson decay modes. From the experimental upper limit for the decay $\bar{B}^0 \to \pi^+\pi^-$ [1] we find a bound for the unknown Kobayashi-Maskawa matrix element $|V_{ub}|$. The difference between D^0 and D^+ lifetimes arises – at least partly – already from the bulk of two-body decay modes. We will discuss this point in Sect. 6. In the final chapter we will summarize our results.

2. Flavour Flow in Nonleptonic Decays

The various ways in which flavour quantum numbers are changed and transmitted in nonleptonic decays allow a classification of the transition amplitudes [11]. We illustrate this in the example of the decay of a charmed meson $(c\bar{q})$. The short distance QCD improved effective interaction is [12]

$$L_{\text{eff}} = \frac{G}{\sqrt{2}} \{C_1(\mu)(\bar{u}d')(\bar{s}'c) + C_2(\mu)(\bar{s}'d')(\bar{u}c)$$
$$+ 4 \text{ quark operators corresponding to penguin typ diagrams} + \text{h.c.}\}$$
$$d' = \cos(\Theta)\, d + \sin(\Theta)\, s$$
$$s' = \cos(\Theta)\, s - \sin(\Theta)\, d$$
$$C_1(\mu) = \frac{C_+ + C_-}{2} \qquad C_2(\mu) = \frac{C_+ - C_-}{2}. \tag{1}$$

Here Θ denotes the Cabibbo angle. The remaining mixing angles are very small and do not have to be considered in charm decays. For the QCD coefficients

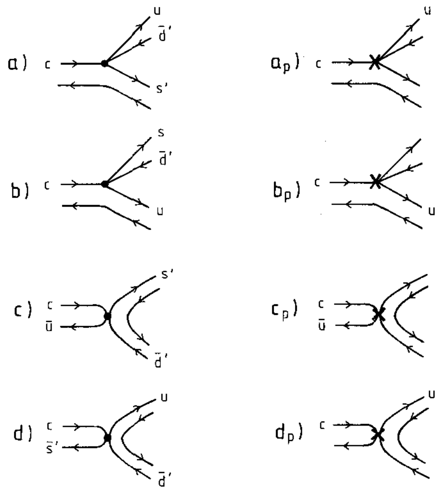

Fig. 1a–d. Flavour flow diagrams for nonleptonic D- and D_s-decays into two mesons. **a** and **b** describe "quark decay" **c** and **d** "quark annihilation" processes. Lines without a name can carry any flavour quantum number and refer to left and right handed fields. In the graphes coming from Penguins $\mathbf{a_p}$ to $\mathbf{d_p}$ the corresponding effective 4 quark interaction is denoted by a cross. Note that the Lorentz structure for $\mathbf{c_p}$ and $\mathbf{d_p}$ is different

C_1 and C_2 one expects at the scale $\mu \approx 1.5$ GeV [13]

$$C_1 \simeq 1.21 \qquad C_2 \simeq -0.42. \tag{2}$$

The flavour flow diagrams for D- and D_s-decays to two final hadrons are shown in Fig. 1. In the diagram of Fig. 1a one of the final mesons is charged and obtains the $\bar{u}d$ or $\bar{u}s$ flavour quantum numbers. In Fig. 1b one of the final mesons carries the quantum number of $\bar{s}d$, $\bar{s}s$, $\bar{d}d$ or $\bar{d}s$. Figures 1c and d describe "annihilation" amplitudes where the two final quarks fragment into hadrons. It should be noted that in general the amplitudes a to d can obtain contributions from both terms in (1). For completeness we also show in Fig. 1 the corresponding flavour flow due to the famous Penguin contributions which arise from loop graphs [14, 15]. They are relevant for Cabibbo suppressed decays only.

Unfortunately, amplitudes with identical flavour flow still depend on the specific initial and final hadron states. Although the QCD forces are flavour independent, they are strongly spin dependent. Moreover the different quark masses generate significant flavour symmetry violations in several direct and indirect ways. Thus, the different couplings, decay constants and final state interaction and nonperturbative effects must be taken into consideration.

3. The Factorization Approach

Nonleptonic decays are notoriously difficult to handle. The $|\Delta\vec{I}| = 1/2$ enhancement in strange particle decays has never been understood in a satisfactory way. For energetic two-body decays of heavy mesons the situation might be somewhat simpler, however [16]. Here the direct generation of a final meson by a quark current is possibly a useful approximation.

The currents are – according to the current-field identities – proportional to interpolating stable or quasistable hadron fields [17]. The approximation now consists in taking, for one current of the current product, only the asymptotic part of the full hadronic field, i.e. its "in" or "out" field. Then the weak amplitude factorizes [18] and is fully determined by the hadron matrix element of the other current. With this replacement of interacting fields by asymptotic fields one neglects, of course, any initial or final state interaction of the corresponding particles. It has been emphasized in particular by Buras et al. [19] that factorization follows to leading order in an $1/N$ expansion where N is the number of quark colours. This argument provides some theoretical justification for the factorization approach.

Thus writing the effective interaction in the form of a Wick ordered product of hadronic currents one gets

$$L_{\text{eff}} = \frac{G}{\sqrt{2}} :\{a_1 (\bar{u} d')_H (\bar{s}' c)_H + a_2 (\bar{s}' d')_H (\bar{u} c)_H\}: \tag{3}$$

The index H indicates the change to hadron field operators in the way described above. We kept the current times current form and omitted Penguin type contributions. Instead of the scale dependent coefficients C_1, C_2 of (1) new scale independent coefficients a_1, a_2 had to be introduced. They are real by time reversal invariance. One expects a relation between a_1, a_2 and the coefficients C_1, C_2. By assuming factorization of (1) at the scale of the decaying heavy quark one finds

$$a_1 \simeq C_1 + \xi\, C_2|_{\mu \simeq m_c, m_b} \qquad a_2 \simeq C_2 + \xi\, C_1|_{\mu \simeq m_c, m_b}. \tag{4}$$

The colour factor $\xi = 1/N$ arises from the colour mismatch in forming colour singlets after Fierz transformation. However, (4) with the value $\xi = 1/3$ cannot be trusted because of the uncertain contribution of colour octet current products obtained by the Fierz transformation [20]. In the following we take a_1 and a_2 as free parameters and later come back to (4). All we need now for the evaluation of nonleptonic decays in the factorization approximation are the meson decay constants and current matrix elements. The amplitude for the process $D^0 \to K^- \pi^+$, for instance, is obtained from (3) with $(\bar{u} d)^\mu_H \Leftrightarrow -f_\pi\, \partial^\mu \phi_{\pi^-} + \ldots \simeq -f_\pi\, \partial^\mu \phi^{\text{out}}_{\pi^-} + \ldots$ which gives

$$A(D^0 \to K^- \pi^+) = \frac{G}{\sqrt{2}} \cos^2(\Theta)\, a_1 (-i f_\pi)\, p^\pi_\mu \cdot \langle K^- | (\bar{s} c)^\mu | D^0 \rangle |_{q^2 = m^2_\pi}. \tag{5}$$

We can distinguish 3 classes of decays: decays determined by a_1 only (class I), decays determined by a_2 only (class II) and decays where a_1 and a_2 amplitudes interfere (class III). Factorization can thus be tested in many ways provided the current matrix elements are known with some confidence. Another feature of the factorization approximation is that "quark annihilation" (Fig. 1c, d) is generally a small correction. There, current matrix elements (in fact the divergence of currents of the lighter quarks) are needed at momentum transfer $q^2 = m^2_D$, $m^2_{D_s}$, m^2_B where the relevant formfactors are expected to be quite small (see Sect. 5). In Tables 9–13 of the appendix we give an extensive list of transition amplitudes in the factorization approximation in terms of a_1 and a_2. The current matrix elements at zero momentum transfer have been calculated as in [3] using relativistic oscillator wave functions. The corresponding formfactors at $q^2 = 0$ are presented in Table 14. For simplicity a pole ansatz with pole masses given in Table 15 is taken for the q^2 dependence of the formfactors. The decay constants used are presented in Table 16. In the computation of Tables 9–13 "annihilation" and final state interaction were neglected. Therefore a comparison of Tables 9–13 with the experimental data must be done with care. We know from experiment [9] that final state interaction cannot be neglected. Indeed, an isospin analysis (next section) shows significant phase differences between $I = 1/2$ and $I = 3/2$ amplitudes at the mass of the D-meson. Nevertheless, and in view of the theoretical uncertainties and approximations quite surprisingly, the experimental decay widths agree roughly [3, 8] with the naive expectation from Tables 9–11. In particular the relative rates within each class of transitions are reasonably well reproduced. The relative signs of a_1 and a_2 can be obtained from class III transitions where a_1 and a_2 amplitudes interfere. In $D \to PP$ transitions (P: pseudoscalar nonet π, K ...) the relevant combination is of the form $a_1 + x a_2$ with $x = +1$ in the $SU(3)$ symmetry limit. $x = +1$ also holds in $D \to PV$ transitions (V: nonet of vector mesons) if the decay constants and matrix elements of P and V are related by collinear $SU(6)$, which combines $SU(3)$ symmetry with spin. (For $D^+ \to PV$ transitions an incorrect V-spin argument leading to $x = -1$ was given in literature. Unfortunately, this argument was accepted by several authors even though it contradicted previous correct calculations.) The D^+-decay rates immediately show that the amplitudes interfere destructively. With $x \approx +1$ this gives

$a_2/a_1<0$ in agreement with what is expected from (4). An indication for $a_2/a_1<0$ was already found in a very early analysis of D-decay data [21].

4. The Effect of Final State Interaction

Final state interaction can seriously affect the decay processes [22]. The D-meson mass lies in a resonance region where rescattering effects of the outgoing mesons will be of particular importance. B-decays may be less influenced, but so far most data are from D-decays. For on-mass-shell final state interactions the bare amplitudes A^0 should be corrected according to the equation

$$A=S^{1/2}A^0 \tag{6}$$

where $S^{1/2}$ denotes the square root of the strong interaction S-matrix for hadron-hadron scattering. Equation (6) induces phasefactors and mixings of channels having the same quantum numbers. Since little is known about the many open channels $S^{1/2}$ cannot be estimated, however. Nevertheless, an isospin analysis gives some information about the effect of final state interaction. In the decays $D\to K\pi$, for instance, the relative phases of amplitudes to $I=1/2$ and $I=3/2$ final states can be obtained directly from the measurements. The isospin decomposition gives

$$\begin{aligned} A(D^0\to K^-\pi^+)&=\frac{1}{\sqrt{3}}(\sqrt{2}\,A_{1/2}+A_{3/2})\\ A(D^0\to \bar K^0\pi^0)&=\frac{1}{\sqrt{3}}(-A_{1/2}+\sqrt{2}\,A_{3/2})\\ A(D^+\to \bar K^0\pi^+)&=\sqrt{3}\,A_{3/2}\\ A_I&=|A_I|\exp(i\delta_I). \end{aligned} \tag{7}$$

Squaring these expressions and using MARK III [9] and lifetime data [23] one finds

$$\begin{aligned} |A_{1/2}|&\simeq(3.35\pm0.19)\,10^{-6}\ \text{GeV}\\ |A_{3/2}|&\simeq(0.99\pm0.38)\,10^{-6}\ \text{GeV}\\ \delta_{1/2}-\delta_{3/2}&\simeq(77\pm11)^\circ. \end{aligned} \tag{8}$$

The individual rates – especially those of class II transitions – are modified by final state interaction. For instance $\Gamma(D^0\to\bar K^0\pi^0)$ would decrease by a factor of 3 if we set $\delta_{1/2}-\delta_{3/2}=0$ keeping $|A_{1/2}|$, $|A_{3/2}|$ fixed.

The isospin analysis (7) can now be used to obtain values for our coefficients a_1, a_2. With the factorization assumption for the *bare* amplitudes A^0 and by allowing only little inelastic effects* we obtain from (7), (8) and Tables 9–11

Table 1. $I=1/2$ and $I=3/2$ amplitudes for $D\to\bar K\rho$ and $D\to\bar K^*\pi$. a_1 and a_2 are taken from $D^0\to\bar K\pi$. The units are 10^{-12} GeV^2

Decay	$\lvert A_{1/2}\rvert^2_{\text{Th}}$	$\lvert A_{1/2}\rvert^2_{\text{Exp}}$	$\lvert A_{3/2}\rvert^2_{\text{Th}}$	$\lvert A_{3/2}\rvert^2_{\text{Exp}}$
$\bar K\rho$	21.1±2.1	24.5±3.6	4.7 ±1.3	3.4±0.9
$\bar K^*\pi$	9.3±1.1	16.5±3.2	$0.08^{+0.80}_{-0.08}$	0.8±0.5
$\bar K\rho+\bar K^*\pi$	30.4±3.2	41.0±4.8	$4.8^{+2.1}_{-1.4}$	4.2±1.0

$$\frac{a_2}{a_1}\simeq-(0.4\pm0.1) \tag{9}$$

and individually (but with correlated errors)

$$a_1\simeq1.3\pm0.1\qquad a_2\simeq-0.55\pm0.1. \tag{10}$$

The ratio a_2/a_1 is not close to -1 which would imply perfect $SU(3)$ sextet dominance [24, 25] for Cabibbo allowed transitions. The negative sign of a_2/a_1 leads to destructive interference in important exclusive D^+ decays as expected from the QCD coefficients C_1, C_2 in (4) [16, 25].

The isospin decomposition as given in (7) also holds for the pseudoscalar-vector (PV) decays $D\to\bar K\rho$ and $D\to\bar K^*\pi$. The cosines of the phase difference $\delta_{1/2}-\delta_{3/2}$ in this case are (again using MARK III data) $0.90^{+0.10}_{-0.22}$ and $0.68^{+0.32}_{-0.46}$ respectively. Unfortunately, the channels $\bar K\rho$ and $\bar K^*\pi$ can mix by final state interaction. They are also connected to the two vector particle state $\bar K^*\rho$, and the $I=1/2$ amplitudes can additionally communicate with $\bar K^0\omega$, $\bar K^{*0}\eta$ and $\bar K^0\phi$. Neglecting all these mixings is certainly not justified, but the corresponding result nevertheless is of some interest. Using a_1 and a_2 from Eq. (10) the calculated $I=1/2$ and $I=3/2$ amplitudes are compared with the experimental results in Table 1. The trend of the data is reproduced but still allows for sizeable mixing effects. If we consider the sums $|A_I^{\bar K\rho}|^2+|A_I^{\bar K^*\pi}|^2$ as presented in the last line of Table 1 the agreement improves as one expects from the unitarity of $S^{1/2}$: in the sum the mixing between $\bar K\rho$ and $\bar K^*\pi$ is inessential if mixing to other channels can be neglected.

* We assume
$|\langle(\bar K\pi)_{I=3/2}|S^{1/2}|(\bar K\pi)_{I=3/2}\rangle|=1$
$|\langle(\bar K\pi)_{I=1/2}|S^{1/2}|(\bar K\pi)_{I=1/2}\rangle|=0.9$ *to* 1
$|\langle(\bar K\eta)|S^{1/2}|(\bar K\pi)_{I=1/2}\rangle|\leq0.4$
and $|\langle(\bar K^*\rho)_{I=1/2}|S^{1/2}|(\bar K\pi)_{I=1/2}\rangle|\simeq0$

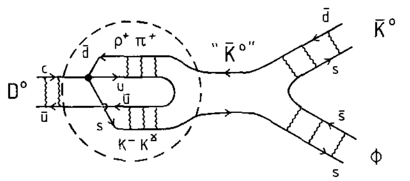

Fig. 2. "Quark annihilation" from "quark decay" and subsequent final state interaction in the process $D^0 \to \bar{K}^0 \phi$. The dotted region describes the subprocess $D^0 \to$ "$\bar{K}^0$" where the "$\bar{K}^0$" states carry the quantum numbers of a $\bar{K}^0$-meson

Amplitudes which are small before final state interactions (especially bare amplitudes proportional to a_2) may receive important contributions via mixing with stronger coupled channels. A case in point is the decay $D^0 \to \bar{K}^0 \phi$ [26] recently taken up by Donoghue [27]. The corresponding amplitude is a pure annihilation amplitude (Fig. 1c) which is very small in the factorization approximation. But this amplitude can be fed through other $I=1/2$ channels. Donoghue suggested the chain $D^0 \to \bar{K}^{*0} \eta \Leftrightarrow \bar{K}^0 \phi$. In our scheme however, the bare amplitude $D^0 \to \bar{K}^{*0} \eta$ is proportional to a_2 (class II) and thus small. The decay chains $D^0 \to (\bar{K}\rho)_{I=1/2} \Leftrightarrow \bar{K}^0 \phi$ and $D^0 \to (\bar{K}^* \pi)_{I=1/2} \Leftrightarrow \bar{K}^0 \phi$ involve stronger transitions because the weak part is proportional to a_1 and therefore larger. The diagram for this process is shown in Fig. 2. With respect to flavour flow it is an annihilation diagram but the annihilation occurs at the strong vertex and thus at the time scale of strong interaction. Such a process will be enhanced if one of the intermediate states "$\bar{K}^0$" with quantum numbers of a $\bar{K}^0$-meson is a resonance in the energy region of the D-mass.

If the transition $D^0 \to \bar{K}^0 \phi$ is indeed caused by rescattering effects one expects an even bigger contribution to the other $I=1/2$ channels $\bar{K}^0 \omega$ and $\bar{K}^{*0} \eta$ because of the larger p-wave phase space in these cases. Without final state interaction and without annihilation one finds from Table 9 taking $|a_2| \simeq 0.55$ $\mathrm{Br}(D^0 \to \bar{K}^0 \omega) \simeq 0.3\%$ while the experimental number is about 4%. Channel mixing alone as inferred from $D^0 \to$ "$\bar{K}^0$" $\to \bar{K}^0 \phi$ and applying $SU(3)$ already predicts $\mathrm{Br}(D^0 \to \bar{K}^0 \omega) \simeq 2\%$ or even more if the creation of the $d\bar{d}$ pairs is favoured with respect to the creation of the $s\bar{s}$ pair in Fig. 2. A similar situation might occur for the decay $D^0 \to \bar{K}^0 \eta$. The factorized transition amplitude is too small but could be fed by the chain $D^0 \to (\bar{K}\pi)_{I=1/2} \Leftrightarrow \bar{K}^0 \eta$.

5. Weak Annihilation Contributions

Apart from the remarks on $D^0 \to \bar{K}^0 \phi$ we considered so far only flavour flows in which the heavy quark decays while the remaining antiquark acts as a spectator. Processes in which heavy and light quarks annihilate and two new quarks are created (Fig. 1c, d) are called annihilation processes. In the factorization approximation the corresponding amplitudes are small since they involve the divergence of currents formed by the lighter quarks and thus go to zero in the limit of vanishing light quark masses. Furthermore, the current divergence is to be taken at $q^2 = m_D^2$, $m_{D_s}^2$, m_B^2i.e. values which are large compared to the quark masses in the decay products. Since all currents are presumably asymptotically (for large q^2) conserved the corresponding contribution is expected to be very small [16]. However, the presence of soft gluons inside hadrons can lead to momentum and angular momentum exchange between gluons and quarks and thus vitiate the helicity suppression of factorized amplitudes [28]. This provides a mechanism which can enhance the annihilation amplitudes and could contribute to the $D^0 - D^+$ lifetime differences. It is of great interest to know to what extend the annihilation process is important, and in particular to what extend it affects two-body decays. The decay $D^0 \to \bar{K}^0 \phi$ can only proceed via annihilation of the valence quarks and the subsequent creation of a strange quark-antiquark pair [29] as is easily seen from the flavour flow diagrams (Fig. 1). The recent discovery of this process [26] has therefore been interpreted as a signal for weak annihilation in D-decays [30].

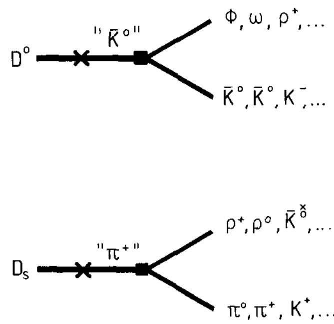

Fig. 3. Cabibbo allowed annihilation diagrams at the hadron level. The cross denotes the weak transitions to virtual states with the quantum numbers of $\bar{K}^0$ in D^0-decays and to virtual states with the quantum numbers of π^+ in D_s^+-decays which then decay strongly

On the level of hadrons the relevant graphs for Cabibbo allowed annihilation transitions to vector and pseudoscalar mesons are shown in Fig. 3. Here the annihilation processes $D^0 \to$ "$\bar{K}^0$", $D_s^+ \to$ "π^+" are followed by decays caused by strong interaction. Before taking these graphs into account we remark that hadron diagrams in which the strong vertex *proceeds* the weak vertex (Fig. 4) are with regard to quark topology decay graphs and not annihilation graphs. More important, the corresponding contribution from heavy intermediate states already are contained in the factorization approach as a form factor effect.

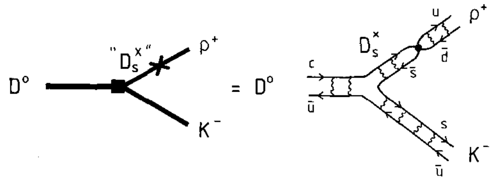

Fig. 4. Decay graph on the level of hadrons. The strong vertex ■ proceeds the weak transition. The cross denotes the subsequent weak vertex. The flavour flow has quark decay topology (the $\bar{u}$ quark acts as a spectator)

The experimentally observed branching ratio for $D^0 \to \bar{K}^0 \phi$ is $\simeq 1\%$. Taking this number as an input value one can easily calculate the "annihilation" contribution to the other channels shown in Fig. 3a since they are all related by $SU(3)$. An immediate conclusion is that "annihilation" is certainly not a dominant mechanism in $D^0 \to K^- \rho^+$ and $D^0 \to \bar{K}^{*-} \pi^+$ decays: the corresponding amplitudes from Fig. 3a are too small to fit the data. However using the graph of Fig. 3a for $D^0 \to \bar{K}^0 \phi$ with the $\bar{K}^0$ (498 MeV)-meson as an intermediate state the fitted value for $\langle \bar{K}^0 | H_W | D^0 \rangle$ is very big [31]. If a similar large number would hold for the amplitude $\langle \pi^+ | H_W | D_s^+ \rangle$ the branching ratios for the decay modes $D_s^+ \to \rho^0 \pi^+$, $\rho^+ \pi^0$ would be large. This would be very interesting but is improbable. It seems more likely to us that the processes of Fig. 3a proceed via a high lying resonance "$\bar{K}^0$" and therefore are enhanced. Such states could be produced directly through the weak Hamiltonian (direct annihilation) if the decay constants f_D and $f_{``K"}$ defined in correspondance to the $\pi$-meson decay constant $f_\pi$ are large enough. The corresponding amplitude is then proportional to $a_2 f_D f_{``K"}$. These states can, however, also be produced in the rescattering process as discussed in Sect. 4 and pictured in Fig. 2. In the latter case the weak amplitude is proportional to a_1 instead of a_2 and thus automatically favoured. Now the cross in Fig. 3a which connects the D-meson with the states "$\bar{K}^0$" stands for the dotted region in Fig. 2. In this case large decay constants are not required.

In any case, for $D \to PV$ decays we have to add to the $I = 1/2$ amplitudes obtained from factorization a piece corresponding to Fig. 3a. The magnitude of this additional amplitude is fixed by the $D^0 \to \bar{K}^0 \phi$ branching ratio, its phase needs an assumption. In a recent article Lusignole and Pugliese [32] also pointed out the necessity of a resonance contribution to $D \to PV$ decays and identified it with the indication for such a resonance as reported in [33]. The resonance parameters are $M(``\bar{K}") \simeq 1830$ MeV and $\Gamma \simeq$ 250 MeV. We take this suggestion, use the Breit Wigner formula and thus find for the phase α of this annihilation amplitude (taking the factorized amplitude real) $|\tan \alpha| \simeq 3.7$. There still is a sign ambiguity in the real part to be removed before we can get the magnitude of the $I = 1/2$ amplitude from the sum of factorization and annihilation amplitudes. Here we simply use that sign which gives good agreement for the $D^0 \to \rho^+ K^-$ width, a transition which is well measured and sensitive to the sign. The relative phases between $I = 1/2$ and $I = 3/2$ amplitudes are taken from the isospin analysis as described in Sect. 4. The result is shown in Table 2. From pure factorization we have qualitative agreement except for $D^0 \to \bar{K}^0 \phi$ and $\bar{K}^0 \omega$. The inclusion of the contribution from Fig. 3a with a phase corresponding to a high lying resonance gives perfect agreement. We remark that the parameters a_1, a_2 have not been adjusted here but taken over from $D \to \bar{K} \pi$ decays.

Table 2. Theoretical branching ratios for $D^0 \to PV$

Decay	Br(%) Theory[a]	Br(%) Theory[b]	Br(%) Experiment [9]
$D^0 \to \bar{K}^0 \phi$	0.0	1.0 fitted	$1.1^{+0.7}_{-0.5}$
$D^0 \to \bar{K}^0 \omega$	0.4	2.7	4.2 ± 1.7
$D^0 \to K^- \rho^+$	12.5	13.8	13.0 ± 1.3
$D^0 \to \bar{K}^0 \rho^0$	0.9	1.1	1.4 ± 0.5
$D^0 \to \bar{K}^{*-} \pi^+$	3.7	9.1	7.4 ± 1.3
$D^0 \to \bar{K}^{*0} \pi^0$	1.4	3.9	2.0 ± 0.9
$D^0 \to \bar{K}^{*0} \eta$	0.3	2.5	–

[a] We used factorized amplitudes (Table 9) with $a_1 = 1.3$, $a_2 = -0.55$
[b] The contributions of the graphs of Fig. 3 are included

For $\bar{K}^* \pi$ and $\bar{K} \rho$ final states the experimentally determined isospin phases are taken into account

The idea of annihilation in the final state interaction as the main origin of otherwise small annihilation amplitudes needs to be tested of course. This will be supported though not proven if the resonance at 1830 MeV can be confirmed. A more conclusive testing ground is provided by D_s-decays. Writing for the matrix element of the effective weak interaction (3) which connects D^0 to any $s\bar{d}$ state "$\bar{K}^0$"

$$\langle ``\bar{K}^0" | L_{\rm eff} | D^0 \rangle = \cos^2 \Theta (a_1 B + a_2 A)$$

the corresponding matrix element connecting D_s^+ to the $u\bar{d}$ state "π" (related by $SU(3)$ to "$\bar{K}^0$") is given by

$$(``\pi" | L_{\rm eff} | D_s^+ \rangle = \cos^2 \Theta (a_1 A + a_2 B).$$

As seen from (3) the quantity A receives contributions from direct annihilation of the heavy meson. In the matrix element B, on the other hand, strong interaction must turn the generated hadrons H into the state "$\bar{K}^0$" (or "π") as in Fig. 2. In the expression for the

Table 3. Theoretical branching ratios for $D_s^+ \to PV$

Decay	Br(%) Theory[a]	Br(%) Theory[b]	Br(%) Experiment [35]
$D_s^+ \to \bar{K}^{*0} \bar{K}^+$	1.6	2.4	4.8 ± 2.4
$D_s^+ \to \bar{K}^0 \bar{K}^{*+}$	0.6	0.3	–
$D_s^+ \to \rho^0 \pi^+$	0.0	0.5	–
$D_s^+ \to \pi^0 \rho^+$	0.0	0.5	–
$D_s^+ \to \phi \pi^+$	2.8	2.8	3.3 ± 1.4

[a] We used factorized amplitudes (Table 10) with $a_1 = 1.3$, $a_2 = -0.55$
[b] Annihilation in the final state interaction only (no direct annihilation) as described in the text

annihilation amplitudes for D^0 and D_s^+ it is an essential point that a_1 and a_2 change their role. Using this fact and comparing D^0 with D_s^+ decays we can already exclude the case of a pure direct annihilation process i.e. $B \simeq 0$! Compared to the well measured decay $D^0 \to \bar{K}^0 \phi$ the D_s^+ annihilation channels would win a large p-wave phase space factor *and* in addition a factor $|a_1/a_2|^2$. In this case $D_s^+ \to \rho^+ \pi^0$, $\rho^0 \pi^+$ would completely dominate the D_s^+-decays and also the branching ratio $D_s^+ \to \bar{K}^{*0} K^+$ would be more than twice its observed value. The opposite extreme, annihilation in the final state interaction process ($B \neq 0$) and very little direct annihilation ($A \simeq 0$) remains as an interesting possibility. The large p-wave phase space factor for $D_s^+ \to \rho \pi$ is then almost compensated by the factor $|a_2/a_1|^2$. This alternative therefore gives branching ratios for $D_s^+ \to \rho \pi$ of roughly 1%. More detailed predictions depend on wether or not $\bar{K}^0(1830)$ and $\pi^+(1770)$ [34] exist. Column 3 of Table 3 has been calculated assuming the relevance of these resonances, taking $\Gamma_{\pi''} \approx 300$ MeV and setting $\mathrm{Br}(D^0 \to \bar{K}^0 \phi) = 1\%$. From the above discussion and the results of Table 3 it is evident that good experimental values or limits for $D_s^+ \to \rho \pi$ will be very helpful to clarify the role of annihilation in two-body decays. Branching ratios $D_s^+ \to \rho \pi$ much larger than presented in Table 3 would indicate the presence of direct annihilation contributions. Branching ratios close to the ones given in Table 3 or smaller would show that the observed annihilation amplitude in $D^0 \to \bar{K}^0 \phi$ is mainly the result of a final state interaction process. In Table 3 one can notice an increase of $\mathrm{Br}(D_s^+ \to \bar{K}^{*0} \bar{K}^+)$ compared to the pure factorization result (column 2) in better agreement with the data. But even without any annihilation an enhanced rate should occur for this process through the chain $D_s^+ \to \phi \rho, \eta \rho \Leftrightarrow \bar{K}^{*0} K^+$ with quark exchange scattering in the final state [8].

In regions far outside any resonances we expect no important annihilation and channel mixing effects. The decay $\bar{B}^0 \to D^{*+} \pi^-$ for instance (Table 12) should be such a case, although mixing with $D^* \rho$ (and $D^{*0} \pi^0$ of course) cannot be excluded. We conclude this section with the remark that inspite of the 1% branching ratio for $D^0 \to \bar{K}^0 \phi$ direct weak annihilation could still be of minor importance in energetic two-body decays.

6. Results and Predictions

We are now in a position to present our complete results and to compare them with the numerous branching ratios now available.

D- and D_s-Decays

For the calculation of the theoretical branching ratios of the factorized amplitudes we used decay constants, polemasses and the $q^2 = 0$ values of the various formfactors given in Tables 14–16 of the appendix. For the lifetimes we used $\tau_{D^0} = (4.4 \pm 0.4) \cdot 10^{-13}$ s, $\tau_{D^+} = (9.25 \pm 1.0) \cdot 10^{-13}$ s and $\tau_{D_s^+} = (3.5 \pm 1.0) \cdot 10^{-13}$ s. The parameters a_1 and a_2 have been fixed from $D \to \bar{K} \pi$ decays where we expect little inelasticity and annihilation and where the isospin phase difference $\delta_{I=1/2} - \delta_{I=3/2}$ is rather well determined. The result for a_1, a_2 was quoted in (9) and (10). In Fig. 5a and Tables 2, 3 and 4a the results for Cabibbo allowed D- and D_s-decays is presented and compared with the experimental branching ratios (with error bars corresponding to statistical errors only). Isospin phase shifts are only taken into account for $D \to \bar{K} \pi$, $D \to \bar{K} \rho$ and $D \to \bar{K}^* \pi$ transitions. Typical theoretical errors due to the various input parameters in particular a_1, a_2 and the errors of the phases range from 20 to 40%. Cabibbo suppressed decays are presented in Fig. 5b and Table 4b.

The overall agreement between the theoretical and experimental numbers is quite remarkable considering the simplicity of the model and the fact that D-decays occur in a resonance region. Taking into account resonance enhanced annihilation contributions improves the agreement with data for some important Cabibbo allowed $D^0 \to PV$ decays (Table 2, column 3). A comparison of D_s^+-decays to $\rho \pi$ with the decay $D^0 \to \bar{K}^0 \phi$ will greatly help to understand the annihilation mechanism.

For Cabibbo suppressed decays the experimental number for the ratio $D^0 \to K^+ K^- / D^0 \to \pi^+ \pi^-$ is 3.8 ± 1.4 in disagreement with the prediction $\simeq 1.4$ from the factorization approach. Since in PP decays annihilation is of minor minor importance this discrepancy may indicate strong final state interaction effects or Penguin type contributions [37] which are, however, difficult to evaluate in this case.

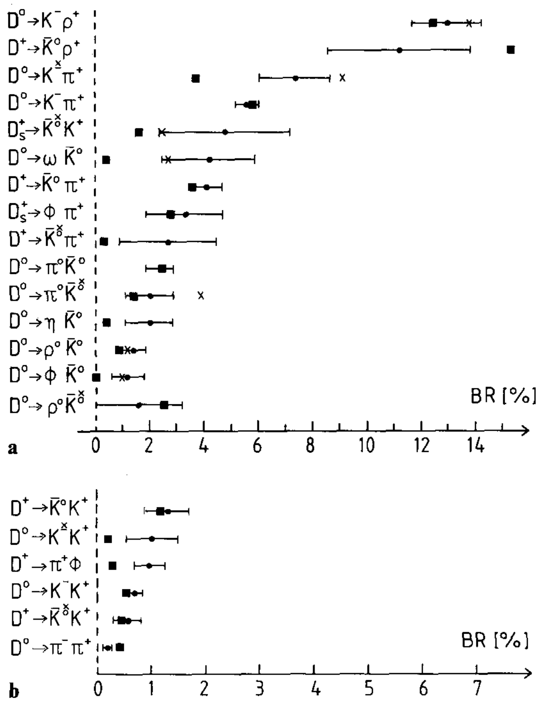

Fig. 5a, b. Comparison between experimental and theoretical branching ratios for D- and D_s-decays. Only statistical errors are indicated. The theoretical values denoted by ■ are from factorized amplitudes with $a_1 \simeq 1.3$ and $a_2 \simeq -0.55$. The branching ratios marked by a cross include "annihilation" as described in the text. **a** Cabibbo allowed D- and D_s-decays. **b** Cabibbo suppressed D-decays

Table 4a. Branching ratios for Cabibbo allowed D- and D_s-decays

Decay	Br(%) Theory	Br(%) Experiment [9]
$D^+ \to \bar{K}^0 \rho^+$	15.3	11.2 ± 2.6
$D^+ \to \bar{K}^0 \pi^+$	3.6	4.1 ± 0.6
$D^+ \to \bar{K}^{*0} \pi^+$	0.3	2.7 ± 1.8
$D^0 \to K^- \pi^+$	5.8	5.6 ± 0.4
$D^0 \to \bar{K}^0 \pi^0$	2.5	2.4 ± 0.5
$D^0 \to \bar{K}^0 \eta$	0.4	2.0 ± 0.9
$D^0 \to \bar{K}^{*0} \rho^0$	2.5	1.6 ± 1.6 [36]

The theoretical numbers represent the expectation from factorization only. $a_1 \simeq 1.3$ and $a_2 \simeq -0.55$ are fixed by the $K\pi$ data

Table 4b. Branching ratios for Cabibbo suppressed D-decays

Decay	Br(%) Theory	Br(%) Experiment [9]
$D^0 \to K^{*-} K^+$	0.21	1.02 ± 0.47
$D^0 \to \pi^+ \pi^-$	0.39	0.18 ± 0.06
$D^0 \to K^- K^+$	0.56	0.68 ± 0.11
$D^+ \to \bar{K}^0 K^+$	1.18	1.30 ± 0.40
$D^+ \to \bar{K}^{*0} K^+$	0.44	0.56 ± 0.25
$D^+ \to \pi^+ \phi$	0.28	0.97 ± 0.27

The theoretical numbers displayed in column 2 correspond to factorization contributions only. $a_1 \simeq 1.3$ and $a_2 \simeq -0.55$ are taken from $K\pi$ data

Knowing now the values for a_1 and a_2 we can discuss the relation of these parameters with the QCD coefficients C_1 and C_2. The numerical comparison shows [8]

$$a_1 \approx C_1(m_c) \qquad a_2 \approx C_2(m_c). \tag{11}$$

Using (4) with $\xi = 1/3$ there is now a large discrepancy between the measured and the naively expected value of a_2. However, $\xi \approx 0$ (corresponding to $N \to \infty$) satisfies simultaneously (4) and (11). Physically, this implies that quarks belonging to *different* colour singlet currents do not combine to form a single meson [8]. Considering our results Buras et al. [19] remarked that factorization together with $\xi \simeq 0$ corresponds to the *lowest* order in the $1/N$ expansion and that it seems to be better to stick to this approximation as long as not all next order corrections are known. Cancellations might occur. Indeed, in the QCD sum rule approach of Blok and Shifman [38] the contribution proportional to $\xi = 1/3$ is practically cancelled by an additional term. Notice, however, that in some particular PV decays Blok and Shifman predict no such compensation. A further study of this point would be very valuable.

We conclude from our experience with D-decays that factorization together with (11) gives generally good results at least for energetic two body decays. The corresponding predictions for D-, D_s- and B-meson decays are presented in Tables 9–13. Especially for weakly coupled channels and for channels to which resonances contribute, corrections for final state interaction and annihilation effects should be taken into account as discussed above. Many not yet measured D-, D_s- and especially B-decay rates can now be predicted with some confidence.

B-Decays

The predictions for various imporant B-decay modes to charmed mesons are given in Table 5a in terms of $|V_{cb}|$. We used $\tau_B \simeq 1.2 \cdot 10^{-12}$ s. Again the values of a_1 and a_2 are of great practical and theoretical interest. What to we expect? The QCD coefficients at the scale of the b-quark mass are [13] $C_1(m_b) \simeq 1.1$ $C_2(m_b) \simeq -0.24$. Once more applying (4) one observes that the value of a_1 is not very sensitive to the colour suppression factor ξ. The value of a_2 on the other hand depends strongly on this colour suppression factor. $\xi \simeq 1/3$ would practically give $a_2 = 0$. From our experience in D-decays we expect, however,

$$a_1 \approx C_1(m_b) \simeq 1.1 \qquad a_2 \approx C_2(m_b) \simeq -0.24 \tag{12}$$

using $\xi \simeq 0$.

Table 5a. Predicted branching ratios for B-decays. We used $a_1 \simeq 1.1$, $a_2 \simeq -0.24$ and $\tau_B \simeq 1.2 \cdot 10^{-12}$ s

Decay	Br(%) Theory	Br(%) Experiment [39]
$\bar{B}^0 \to D^+\pi^-$	$0.6\,(V_{cb}/0.05)^2$	$0.14 \pm 0.19 \pm 0.05$
$\bar{B}^0 \to D^{*+}\pi^-$	$0.5\,(V_{cb}/0.05)^2$	$0.25 \pm 0.15 \pm 0.15$
$\bar{B}^0 \to D^{*+}\rho^-$	$1.5\,(V_{cb}/0.05)^2$	
$\bar{B}^0 \to D^{*+}A_1^-$	$1.9\,(V_{cb}/0.05)^2$	
$\bar{B}^0 \to D^{*+}D_s^{*-}$	$2.4\,(V_{cb}/0.05)^2$	
$\bar{B}^0 \to \bar{K}^0 J/\Psi$	$0.06\,(V_{cb}/0.05)^2$	
$\bar{B}^0 \to \bar{K}^{*0} J/\Psi$	$0.25\,(V_{cb}/0.05)^2$	0.44 ± 0.27
$B^- \to D^0\pi^-$	$0.4\,(V_{cb}/0.05)^2$	$0.38 \pm 0.14 \pm 0.11$
$B^- \to D^0\rho^-$	$1.3\,(V_{cb}/0.05)^2$	
$B^- \to D^{*0}\pi^-$	$0.3\,(V_{cb}/0.05)^2$	
$B^- \to D^{*0}\rho^-$	$1.0\,(V_{cb}/0.05)^2$	
$B^- \to D^0 D_s^-$	$0.8\,(V_{cb}/0.05)^2$	
$B^- \to D^0 D_s^-$	$0.9\,(V_{cb}/0.05)^2$	
$B^- \to D^{*0} D_s^-$	$2.4\,(V_{cb}/0.05)^2$	
$B^- \to D^{*0} D_s^{*-}$	$0.4\,(V_{cb}/0.05)^2$	
$B^- \to K^- J/\Psi$	$0.06\,(V_{cb}/0.05)^2$	$0.09 \pm 0.06 \pm 0.02$
$B^- \to K^{*-} J/\Psi$	$0.25\,(V_{cb}/0.05)^2$	
$B^- \to \rho^- J/\Psi$	$0.01\,(V_{cb}/0.05)^2$	

For the decay constants the values given in Table 16 are used

Table 5b. Predicted branching ratios for B-decays. We used $a_1 \simeq 1.1$, $a_2 \simeq -0.24$, $|V_{cb}| \simeq 0.05$ and $\tau_B \simeq 1.2 \cdot 10^{-12}$ s

Decay	Br(%) Theory	Br(%) Experiment [1]
$\bar{B}^0 \to \pi^+\pi^-$	$0.21\,(V_{ub}/V_{cb})^2$	$\leqq 0.02$
$\bar{B}^0 \to \pi^+\rho^-$	$0.56\,(V_{ub}/V_{cb})^2$	
$\bar{B}^0 \to \pi^+A_1^-$	$0.59\,(V_{ub}/V_{cb})^2$	$\leqq 0.24$
$\bar{B}^0 \to \rho^+\rho^-$	$0.45\,(V_{ub}/V_{cb})^2$	
$\bar{B}^0 \to \rho^+A_1^-$	$0.67\,(V_{ub}/V_{cb})^2$	
$\bar{B}^0 \to \rho^0\pi^0$	$0.01\,(V_{ub}/V_{cb})^2$	
$\bar{B}^0 \to \rho^0\rho^0$	$0.01\,(V_{ub}/V_{cb})^2$	
$B^- \to \pi^0\pi^-$	$0.06\,(V_{ub}/V_{cb})^2$	
$B^- \to \pi^0\rho^-$	$0.22\,(V_{ub}/V_{cb})^2$	
$B^- \to \rho^0\pi^-$	$0.06\,(V_{ub}/V_{cb})^2$	$\leqq 0.02$
$B^- \to \rho^0\rho^-$	$0.14\,(V_{ub}/V_{cb})^2$	
$B^- \to \rho^0 A_1^-$	$0.33\,(V_{ub}/V_{cb})^2$	$\leqq 0.08$

Table 6. Predicted branching ratios for B-transitions via Penguin interaction

Decay	Br (%) Theory
$\bar{B}^0 \to \bar{K}^0\phi$	$1.2 \cdot 10^{-5}$
$\bar{B}^0 \to \rho^+K^{*-}$	$7.8 \cdot 10^{-6}$
$\bar{B}^0 \to \pi^0K^{*-}$	$4.4 \cdot 10^{-6}$

As a test for a_1 the decay $\bar{B} \to D^{*+}\pi^-$ can be used. From (12) taking $|V_{cb}| \simeq 0.05$ we predicted [3, 8] a branching ratio of $\simeq 0.5\%$. This number is in agreement with a recent measurement by the ARGUS collaboration [39] which found $\mathrm{Br}(\bar{B} \to D^{*+}\pi^-) \simeq 0.25 \pm 0.15 \pm 0.15\%$. As a test for $|a_2|$ the decay $\bar{B}^0 \to \bar{K}^{*0} J/\Psi$ is suitable. Using (12) we predicted [3, 8] a branching ratio of 0.3%. Recent measurements from CLEO and ARGUS give $\mathrm{Br}(\bar{B}^0 \to \bar{K}^{*0} J/\Psi) \simeq 0.41 \pm 0.19 \pm 0.03\%$ and $0.44 \pm 0.27\%$ [39]. Again, our simple model appears to be surprisingly successful. Necessary additional tests can now be performed. If they are successful, specific decay channels will allow a determination of so far unknown decay constants. For instance the decay $\bar{B}^0 \to D^{*+} D_s^{*-}$ is proportional to $(F_{D_s^{*-}}/F_{\rho^+})^2$ (see Appendix A).

Of great interest of course are B-decays to non charmed and non strange states. They depend on the Kobayashi-Maskawa matrix element $|V_{ub}|$ for which only an upper limit is know. Such transitions can, however, also be induced by the Penguin interaction term proportional to $V_{cd}^* V_{cb}$. The factorization method gives us an orientation about the significance of this latter interaction: For two-body transitions to non charmed and non strange states one finds branching ratios from the standard Penguin graph of the order of only $\approx 3 \times 10^{-7}$. Thus, we will neglect the Penguin diagram here assuming that the matrix element $|V_{ub}|$ is not too small (The standard model requires $|V_{ub}/V_{cb}| \geqq 0.05$ to be able to describe CP-violation in K-decays. Models for the quark mass matrix [40–42] predict $|V_{ub}/V_{cb}| \simeq \sqrt{m_u/m_c} \simeq 0.06$, very close to the lower limit).

In Table 5b our predictions for the branching ratios of several B-decays to non charmed states are displayed. The theoretical numbers proportional to $|V_{ub}|^2$ depend on the square of small overlap factors between the wavefunctions of a very heavy and a light meson. Therefore, the theoretical error can be a factor ≈ 2 but presumably less for the relative rates of these decays. A first restriction for the unknown matrix element $|V_{ub}|$ from exclusive nonleptonic decays can be obtained from the observed limit $\mathrm{Br}(\bar{B}^0 \to \pi^+\pi^-) \leqq 0.02\%$ [1]. Taking into account the above quoted error we obtain the limit $|V_{ub}| \leqq 0.03$.

B-decays to non charmed but strange final states also are of great interest. They are ideally suited to obtain information about the Penguin interaction [43, 44]. In Table 6 we present three relevant branching ratios in factorization approximation taking $(\alpha(\mu_b)/12\pi \times \ln m_t^2/m_c^2) \simeq 0.05$. The decay $\bar{B}^0 \to \bar{K}^0\phi$ can only arise from this interaction. The two remaining rates in Table 6 are expected if the Penguin diagram dominates, i.e. for $|V_{ub}/V_{cb}| \leqq 0.1$.

Exclusive Decays and Lifetime Differences

Exclusive nonleptonic decays not only provide information on QCD coefficients and their relative signs but also shed light on the origin of the lifetime difference between D^0 and D^+ mesons. We have seen in the last section, that at least the energetic two-body transition amplitudes are roughly described by a factorized form of the weak amplitude. Encouraged by these results we computed many more two-body decays* (more than presented in Tables 9–13) and summed them up, in order to estimate their contribution to the nonleptonic decay widths. Naturally, this estimate can at best give an orientation since for transitions with little energy release, for instance $D \to \bar{K}^* \omega$, the factorization approximation is doubtful. Final state interaction effects, on the other hand, cancel to some extent in the sum because of the unitarity of the strong interaction S-matrix.

Using for the parameter a_1, a_2 the values 1.3 ± 0.1 and -0.55 ± 0.1, it turns out that about 70–80% of the total nonleptonic transition rates of D^0 and D^+ are accounted for by two-body decays (Table 7). More important, the calculated ratio $\Gamma(D^0 \to XY)/\Gamma(D^+ \to XY)$ for these nonleptonic two-body decays turned out to be $\simeq 2.7$ (Table 7). Thus a sizeable part of the lifetime difference between D^0 and D^+ arises from two-body decays due to the destructive interference ($a_2/a_1 \leqq 0$) in several important D^+ decays [8]. Note that no annihilation contribution has been used for this estimate.

The corresponding calculations have also been performed for nonleptonic two-body decays of the $\bar{B}^0$ and B^- mesons*. We use for a_1 and a_2 the values displayed in (12). If these numbers are approximately correct, interference effects are small. Thus we do not expect that two-body decays cause a sizeable lifetime difference between $\bar{B}^0$ and B^- decays (see Table 8). Furthermore it turns out that only 10–15% of the total decay rates for B^- and $\bar{B}^0$ involving presently known states can be due to nonleptonic two-body decay channels.

Table 7. Two-body nonleptonic decay widths summed up and compared with the measured total nonleptonic widths for D^0, D^+ and D_s^+ transitions. The units are $10^{10}\,\mathrm{s}^{-1}$

Meson	$\Gamma^{\text{th}}(D \to XY)$	$\Gamma^{\text{Exp}}(D \to \text{nonleptonic})$
D^0	153 ± 22	194 ± 48
D^+	56 ± 15	71 ± 14
D_s^+	126 ± 15	–

* In this calculation we included all particles which belong to a $SU(3)$ pseudoscalar or vector nonet. Also included are A_1 and K_1 particles but only as far as they can be produced directly from the corresponding currents

* Here we included all members of the $SU(4)$ pseudoscalar and vector 15-plet in the final state but also A_1 and K_1 as far as they are produced directly from the corresponding currents

Table 8. Summed up nonleptonic two-body decay rates for $\bar{B}^0$ and B^- mesons. We used $a_1 \simeq 1.1$, $a_2 \simeq -0.24$ and $\tau_B \simeq 1.2 \cdot 10^{-12}$ s. The units are $10^{10}\,\mathrm{s}^{-1}$

Meson	$\Gamma^{\text{Th}}(B \to XY)$	$\Gamma^{\text{Exp}}_{\text{tot}}(B \to \text{all})$
B^-	9.8	83 ± 30
$\bar{B}^0$	12.0	

7. Summary

In the present paper we analyse two-body decay rates of D-, D_s- and B-mesons. Using a factorized form of the weak Hamiltonian we found good agreement with the existing data indicating that quark decay is the dominant mechanism for energetic two-body decays of heavy mesons. The $D \to K\pi$ decay rates measured by the MARK III collaboration have been used to fix the two parameters a_1 and a_2 which we had to introduce in the effective interaction (3). The result $a_1 \approx C_1(m_c)$ and $a_2 \approx C_2(m_c)$ indicates effective total "colour mismatch": $\xi \simeq 0$. In physical terms this means that quarks associated with different colour singlet currents do not easily combine to form a single meson. We calculated the decay widths of practically all two-body decay channels of D^0-, D^+- and D_s^+-mesons into pseudoscalar and vector mesons. We found that a sizeable part of the lifetime difference between D^0 and D^+ arises from two-body decays due to the destructive interference – ($a_2/a_1 < 0$) – in important D^+ decays. Since the D- and D_s-mesons lie in a resonance region we argued that in some decay channels resonances enhance final state interaction effects and otherwise small annihilation contributions. A case in point is the experimentally well established decay $D^0 \to \bar{K}^0 \phi$ where annihilation might occur in the final state interaction. D_s-decays will shed further light on this problem as discussed in Sect. 5: a large branching ratio for $D_s \to \rho\pi$ would indicate a noticeable contribution from the direct weak annihilation process. A smaller but not negligeable branching ratio ($\approx 1\%$) would suggest the occurrence of annihilation in a resonance scattering process after the weak decay.

We give predictions for many two-body B-mesons decay widths. They can be used with some confidence since resonance scattering in the final state is presumably of minor importance in most cases. Our theoretical results are in agreement with the few available experimental data using $a_1 \approx C_1(m_b)$ and $a_2 \approx C_2(m_b)$. If these relations for a_1 and a_2 are supported by further measurements one can conclude that effective total "colour mismatch" also holds at the scale relevant for B-meson decays. A first restriction on the Kobayashi-Maskawa matrix element $|V_{ub}|$ has been obtained from the limit $\mathrm{Br}(\bar{B}^0 \to \pi^+\pi^-) \leqq 0.02\%$. We found $|V_{ub}| \leqq 0.03$.

Acknowledgement. We like to thank Klaus Schubert for many lively discussions. We are also grateful to the German Ministerium für Forschung und Technologie for financial support.

Appendix A. Nonleptonic Widths of D-, D_s- and B-Mesons

Table 9. D^0-decay widths

Decay	Widths in $10^{10}\,\mathrm{s}^{-1}$	Decay	Widths in $10^{10}\,\mathrm{s}^{-1}$
$D^0 \to K^-\pi^+$	$9.92\,a_1^2$	$D^0 \to \eta' \bar{K}^{*0}$	$0.02\,a_2^2$
$D^0 \to K^-\rho^+$	$17.43\,a_1^2$	$D^0 \to \omega \bar{K}^0$	$3.04\,a_2^2$
$D^0 \to K^-A_1^+$	$2.43\,a_1^2$	$D^0 \to \omega \bar{K}^{*0}$	$17.64\,a_2^2$
$D^0 \to K^{*-}\pi^+$	$5.12\,a_1^2$		
$D^0 \to K^{*-}\rho^+$	$34.05\,a_1^2$	$D^0 \to \pi^0\pi^0$	$0.26\,a_2^2$
		$D^0 \to \pi^0\rho^0$	$0.63\,a_2^2$
$D^0 \to \pi^-\pi^+$	$0.52\,a_1^2$	$D^0 \to \pi^0\omega$	$0.06\,a_2^2$
$D^0 \to \pi^-\rho^+$	$1.11\,a_1^2$	$D^0 \to \pi^0 A_1^0$	$0.16\,a_2^2$
$D^0 \to \pi^-A_1^+$	$0.65\,a_1^2$	$D^0 \to \pi^0\eta$	$0.15\,a_2^2$
$D^0 \to \rho^-\pi^+$	$0.28\,a_1^2$	$D^0 \to \pi^0\eta'$	$0.07\,a_2^2$
$D^0 \to \rho^-\rho^+$	$1.89\,a_1^2$	$D^0 \to \pi^0\phi$	$0.49\,a_2^2$
$D^0 \to K^-K^+$	$0.75\,a_1^2$	$D^0 \to \rho^0\rho^0$	$0.95\,a_2^2$
$D^0 \to K^-K^{*+}$	$0.74\,a_1^2$		
$D^0 \to K^{*-}K^+$	$0.28\,a_1^2$	$D^0 \to \rho^0\eta$	$0.01\,a_2^2$
$D^0 \to K^{*-}K^{*-}$	$1.45\,a_1^2$	$D^0 \to \rho^0\eta'$	$0.02\,a_2^2$
		$D^0 \to \rho^0\phi$	$0.82\,a_2^2$
$D^0 \to \pi^0\bar{K}^0$	$7.55\,a_2^2$	$D^0 \to \omega\omega$	$0.87\,a_2^2$
$D^0 \to \pi^0\bar{K}^{*0}$	$9.72\,a_2^2$	$D^0 \to \omega\eta$	$0.43\,a_2^2$
$D^0 \to \rho^0\bar{K}^0$	$3.14\,a_2^2$	$D^0 \to \omega\phi$	$0.74\,a_2^2$
$D^0 \to \rho^0\bar{K}^{*0}$	$18.45\,a_2^2$	$D^0 \to \eta\eta$	$0.29\,a_2^2$
$D^0 \to \eta\bar{K}^0$	$2.86\,a_2^2$		
$D^0 \to \eta\bar{K}^{*0}$	$2.57\,a_2^2$	$D^0 \to \eta\eta'$	$0.03\,a_2^2$
$D^0 \to \eta'\bar{K}^0$	$1.15\,a_2^2$	$D^0 \to \eta\phi$	$0.11\,a_2^2$

Table 10. D_s^+-decay widths

Decay	Widths in $10^{10}\,\mathrm{s}^{-1}$	Decay	Widths in $10^{10}\,\mathrm{s}^{-1}$
$D_s^+ \to \eta\pi^+$	$4.93\,a_1^2$	$D_s^+ \to K^+\pi^0$	$0.22\,a_2^2$
$D_s^+ \to \eta\rho^+$	$9.27\,a_1^2$	$D_s^+ \to K^+\omega$	$0.41\,a_2^2$
$D_s^+ \to \eta A_1^+$	$2.21\,a_1^2$	$D_s^+ \to K^+A_1^0$	$0.16\,a_2^2$
$D_s^+ \to \eta'\pi^+$	$2.89\,a_1^2$	$D_s^+ \to K^{*+}\pi^0$	$0.13\,a_2^2$
$D_s^+ \to \eta'\rho^+$	$2.62\,a_1^2$	$D_s^+ \to K^{*+}\rho^0$	$0.85\,a_2^2$
$D_s^+ \to \phi\pi^+$	$4.72\,a_1^2$	$D_s^+ \to K^{*+}\omega$	$0.80\,a_2^2$
$D_s^+ \to \phi\rho^+$	$29.74\,a_1^2$		
		$D_s^+ \to \eta K^+$	$0.38\,(a_1+1.31\,a_2)^2$
$D_s^+ \to K^0\pi^+$	$0.44\,a_1^2$	$D_s^+ \to \eta K^{*+}$	$0.41\,(a_1+0.82\,a_2)^2$
$D_s^+ \to \bar{K}^0\rho^+$	$0.89\,a_1^2$	$D_s^+ \to \eta' K^+$	$0.21\,(a_1+0.34\,a_2)^2$
$D_s^+ \to K^0A_1^+$	$0.31\,a_1^2$	$D_s^+ \to \eta' K^{*+}$	$0.06\,(a_1+0.19\,a_2)^2$
$D_s^+ \to K^{*0}\pi^+$	$0.26\,a_1^2$	$D_s^+ \to \phi K^+$	$0.26\,(a_1+1.67\,a_2)^2$
$D_s^+ \to K^{*0}\rho^+$	$1.69\,a_1^2$	$D_s^+ \to \phi K^{*+}$	$1.15\,(a_1+1.08\,a_2)^2$
$D_s^+ \to K^+\bar{K}^0$	$12.76\,a_2^2$		
$D_s^+ \to K^+\bar{K}^{*0}$	$15.04\,a_2^2$		
$D_s^+ \to K^{*+}\bar{K}^0$	$5.85\,a_2^2$		
$D_s^+ \to K^{*+}\bar{K}^{*0}$	$32.54\,a_2^2$		

Tables 9 to 13 contain decay widths in the factorization approximation. The formfactors of current matrix elements at $q^2=0$ are calculated as in (3) and are displayed in Table 14. Pole masses for the formfactors are given in Table 15. Class III decays are written in the form $(a_1 + x a_2)^2$. (For VV transitions this form is only approximately correct, the numerical deviation however is very small.) For the decay constants we used the values shown in Table 16. The explicit dependence on the decay onstants is as follows: In a decay $D \to XY$ the amplitude proportional to a_1 (class

Table 11. D^+-decay widths

Decay	Widths in $10^{10}\,\mathrm{s}^{-1}$	Decay	Widths in $10^{10}\,\mathrm{s}^{-1}$
$D^+ \to \bar{K}^0\pi^+$	$9.98\,(a_1+1.23\,a_2)^2$	$D^+ \to \bar{K}^0A_1^+$	$2.49\,a_1^2$
$D^+ \to \bar{K}^0\rho^+$	$17.57\,(a_1+0.60\,a_2)^2$	$D^+ \to \bar{K}^0K^+$	$0.76\,a_1^2$
$D^+ \to \bar{K}^{*0}\pi^+$	$5.18\,(a_1+1.95\,a_2)^2$	$D^+ \to \bar{K}^0K^{*+}$	$0.74\,a_1^2$
$D^+ \to \bar{K}^{*0}\rho^+$	$34.59\,(a_1+1.04\,a_2)^2$		
		$D^+ \to \bar{K}^{*0}K^+$	$0.29\,a_1^2$
$D^+ \to \pi^0\pi^+$	$0.26\,(a_1+1.00\,a_2)^2$	$D^+ \to \bar{K}^{*0}K^{*+}$	$1.50\,a_1^2$
$D^+ \to \pi^0\rho^+$	$0.57\,(a_1+0.50\,a_2)^2$	$D^+ \to \pi^0A_1^+$	$0.33\,a_1^2$
$D^+ \to \rho^0\pi^+$	$0.14\,(a_1+2.00\,a_2)^2$		
$D^+ \to \rho^0\rho^+$	$0.96\,(a_1+1.00\,a_2)^2$	$D^+ \to \pi^+\phi$	$0.99\,a_2^2$
		$D^+ \to \rho^+\phi$	$0.71\,a_2^2$
$D^+ \to \omega\pi^+$	$0.93\,(a_1+0.99\,a_2)^2$		
$D^+ \to \eta\pi^+$	$0.10\,(a_1+2.73\,a_2)^2$		
$D^+ \to \eta\rho^+$	$0.17\,(a_1+1.32\,a_2)^2$		
$D^+ \to \eta'\pi^+$	$0.05\,(a_1-0.80\,a_2)^2$		
$D^+ \to \eta'\rho^+$	$0.02\,(a_1-0.34\,a_2)^2$		

Table 12. $\bar{B}^0$-decay widths. We used $|V_{cb}|=0.05$

Decay	Widths in $10^{10}\,\mathrm{s}^{-1}$	Decay	Widths in $10^{10}\,\mathrm{s}^{-1}$
$\bar{B}^0 \to D^+\pi^-$	$0.40\,a_1^2$	$\bar{B}^0 \to \pi^0D^0$	$0.11\,a_2^2$
$\bar{B}^0 \to D^+\rho^-$	$1.04\,a_1^2$	$\bar{B}^0 \to \pi^0D^{*0}$	$0.16\,a_2^2$
$\bar{B}^0 \to D^+A_1^-$	$1.04\,a_1^2$	$\bar{B}^0 \to \rho^0D^0$	$0.06\,a_2^2$
$\bar{B}^0 \to D^{*+}\pi^-$	$0.31\,a_1^2$	$\bar{B}^0 \to \rho^0D^{*0}$	$0.32\,a_2^2$
$\bar{B}^0 \to D^{*+}A_1^-$	$1.36\,a_1^2$	$\bar{B}^0 \to \eta D^{*0}$	$0.07\,a_2^2$
$\bar{B}^0 \to D^+D_s^-$	$0.56\,a_1^2$	$\bar{B}^0 \to \omega D^0$	$0.06\,a_2^2$
$\bar{B}^0 \to D^+D_s^{*-}$	$0.61\,a_1^2$	$\bar{B}^0 \to \omega D^{*0}$	$0.31\,a_2^2$
$\bar{B}^0 \to D^{*+}D_s^-$	$0.25\,a_1^2$	$\bar{B}^0 \to \eta' D^0$	$0.03\,a_2^2$
$\bar{B}^0 \to D^{*+}D_s^{*-}$	$1.69\,a_1^2$	$\bar{B}^0 \to \eta' D^{*0}$	$0.04\,a_2^2$
$\bar{B}^0 \to D^+K^-$	$0.03\,a_1^2$	$\bar{B}^0 \to \bar{K}^0J/\Psi$	$0.85\,a_2^2$
$\bar{B}^0 \to D^+K^{*-}$	$0.05\,a_1^2$	$\bar{B}^0 \to \bar{K}^{*0}J/\Psi$	$3.63\,a_2^2$
$\bar{B}^0 \to D^{*+}K^-$	$0.02\,a_1^2$	$\bar{B}^0 \to \bar{K}^{*0}D^{*0}$	$0.04\,a_2^2$
$\bar{B}^0 \to D^{*+}K^{*-}$	$0.05\,a_1^2$	$\bar{B}^0 \to \pi^0J/\Psi$	$0.02\,a_2^2$
$\bar{B}^0 \to D^+D^-$	$0.03\,a_1^2$	$\bar{B}^0 \to \rho^0J/\Psi$	$0.08\,a_2^2$
$\bar{B}^0 \to D^+D^{*-}$	$0.03\,a_1^2$	$\bar{B}^0 \to \omega J/\Psi$	$0.08\,a_2^2$
$\bar{B}^0 \to D^{*+}D^-$	$0.01\,a_1^2$		
$\bar{B}^0 \to D^{*+}D^{*-}$	$0.08\,a_1^2$	$\bar{B}^0 \to \pi^0\pi^0$	$0.07\,a_2^2(V_{ub}/V_{cb})^2$
		$\bar{B}^0 \to \pi^0\rho^0$	$0.21\,a_2^2(V_{ub}/V_{cb})^2$
$\bar{B}^0 \to \pi^+\pi^-$	$0.14\,a_1^2(V_{ub}/V_{cb})^2$	$\bar{B}^0 \to \pi^0A_1^0$	$0.10\,a_2^2(V_{ub}/V_{cb})^2$
$\bar{B}^0 \to \pi^+\rho^-$	$0.38\,a_1^2(V_{ub}/V_{cb})^2$	$\bar{B}^0 \to \rho^0\rho^0$	$0.16\,a_2^2(V_{ub}/V_{cb})^2$
$\bar{B}^0 \to \pi^+A_1^-$	$0.41\,a_1^2(V_{ub}/V_{cb})^2$	$\bar{B}^0 \to \rho^0A_1^0$	$0.12\,a_2^2(V_{ub}/V_{cb})^2$
$\bar{B}^0 \to \rho^+\pi^-$	$0.09\,a_1^2(V_{ub}/V_{cb})^2$	$\bar{B}^0 \to \pi^0\omega$	$0.02\,a_2^2(V_{ub}/V_{cb})^2$
$\bar{B}^0 \to \rho^+\rho^-$	$0.31\,a_1^2(V_{ub}/V_{cb})^2$		
$\bar{B}^0 \to \rho^+A_1^-$	$0.46\,a_1^2(V_{ub}/V_{cb})^2$		

Table 13. B^--decay widths. We used $|V_{cb}|=0.05$

Decay	Widths in $10^{10}\,s^{-1}$	Decay	Widths in $10^{10}\,s^{-1}$
$B^- \to D^0\pi^-$	$0.40\,(a_1+0.75\,a_2)^2$	$B^- \to \pi^0\pi^-$	$0.07\,(a_1+1.00\,a_2)^2\,(V_{ub}/V_{cb})^2$
$B^- \to D^0\rho^-$	$1.04\,(a_1+0.34\,a_2)^2$	$B^- \to \pi^0\rho^-$	$0.19\,(a_1+0.50\,a_2)^2\,(V_{ub}/V_{cb})^2$
$B^- \to D^{*0}\pi^-$	$0.31\,(a_1+1.04\,a_2)^2$	$B^- \to \rho^0\pi^-$	$0.05\,(a_1+2.01\,a_2)^2\,(V_{ub}/V_{cb})^2$
$B^- \to D^{*0}\rho^-$	$0.98\,(a_1+0.79\,a_2)^2$	$B^- \to \rho^0\rho^-$	$0.16\,(a_1+1.00\,a_2)^2\,(V_{ub}/V_{cb})^2$
$B^- \to D^0K^-$	$0.03\,(a_1+0.46\,a_2)^2$	$B^- \to \eta\pi^-$	$0.03\,(a_1+1.11\,a_2)^2\,(V_{ub}/V_{cb})^2$
$B^- \to D^0K^{*-}$	$0.05\,(a_1+0.26\,a_2)^2$	$B^- \to \eta\rho^-$	$0.08\,(a_1+0.55\,a_2)^2\,(V_{ub}/V_{cb})^2$
$B^- \to D^{*0}K^-$	$0.02\,(a_1+0.64\,a_2)^2$	$B^- \to \omega\pi^-$	$0.05\,(a_1+1.95\,a_2)^2\,(V_{ub}/V_{cb})^2$
$B^- \to D^{*0}K^{*-}$	$0.05\,(a_1+0.85\,a_2)^2$	$B^- \to \omega\rho^-$	$0.15\,(a_1+0.98\,a_2)^2\,(V_{ub}/V_{cb})^2$
$B^- \to D^0A_1^-$	$1.04\,a_1^2$	$B^- \to \pi^0A_1^-$	$0.21\,a_1^2\,(V_{ub}/V_{cb})^2$
$B^- \to D^{*0}A_1^-$	$1.35\,a_1^2$	$B^- \to \rho^0A_1^-$	$0.23\,a_1^2\,(V_{ub}/V_{cb})^2$
$B^- \to D^0D_s^-$	$0.56\,a_1^2$	$B^- \to \eta A_1^-$	$0.09\,a_1^2\,(V_{ub}/V_{cb})^2$
$B^- \to D^0D_s^{*-}$	$0.61\,a_1^2$	$B^- \to \eta' A_1^-$	$0.05\,a_1^2\,(V_{ub}/V_{cb})^2$
$B^- \to D^{*0}D_s^-$	$0.25\,a_1^2$	$B^- \to \omega A_1^-$	$0.23\,a_1^2\,(V_{ub}/V_{cb})^2$
$B^- \to D^{*0}D_s^{*-}$	$1.68\,a_1^2$		
$B^- \to D^0D^-$	$0.03\,a_1^2$	$B^- \to K^-\bar{D}^0$	$0.28\,a_2^2\,(V_{ub}/V_{cb})^2$
$B^- \to D^0D^{*-}$	$0.03\,a_1^2$	$B^- \to K^-\bar{D}^{*0}$	$0.40\,a_2^2\,(V_{ub}/V_{cb})^2$
$B^- \to D^{*0}D^-$	$0.01\,a_1^2$	$B^- \to K^{*-}\bar{D}^0$	$0.15\,a_2^2\,(V_{ub}/V_{cb})^2$
		$B^- \to K^{*-}\bar{D}^{*0}$	$0.76\,a_2^2\,(V_{ub}/V_{cb})^2$
$B^- \to K^-J/\Psi$	$0.84\,a_2^2$		
$B^- \to K^{*-}J/\Psi$	$3.61\,a_2^2$		
$B^- \to \pi^-J/\Psi$	$0.04\,a_2^2$		
$B^- \to \rho^-J/\Psi$	$0.16\,a_2^2$		

I) or a_2 (class II) scale according to the decay constant of the meson Y. For class III amplitudes the parts proportional to a_1 (a_2) scale according to the decay constant of the meson $Y(X)$.

Appendix B. Formfactors Polmasses and Couplings

Table 14. Formfactors at zero momentum transfer for $P \to P$ and $P \to V$ transitions

Decay	$F_1=F_0$	V	A_1	A_2	$A_3=A_0$
$K \to \pi$	0.992				
$D \to K$	0.762				
$D \to \pi$	0.692				
$D \to \eta$	0.681				
$D \to \eta'$	0.655				
$D \to K^*$		1.226	0.880	1.147	0.733
$D \to \rho$		1.225	0.775	0.923	0.669
$D \to \omega$		1.236	0.772	0.920	0.669
$D_s \to \eta$	0.723				
$D_s \to \eta'$	0.704				
$D_s \to K$	0.643				
$D_s \to K^*$		1.250	0.717	0.853	0.634
$D_s \to \phi$		1.319	0.820	1.076	0.700
$B \to D$	0.690				
$B \to K$	0.379				
$B \to \pi$	0.333				
$B \to \eta$	0.307				
$B \to \eta'$	0.254				
$B \to D^*$		0.705	0.651	0.686	0.623
$B \to K^*$		0.369	0.328	0.331	0.321
$B \to \rho$		0.329	0.283	0.283	0.281
$B \to \omega$		0.328	0.281	0.281	0.280

The numerical calculation is performed as in [3]
This reference also contains our definition of the formfactors

Table 15. Values of pole masses used in the numerical estimates

Current	$m(0^-)$ (GeV)	$m(1^-)$ (GeV)	$m(0^+)$ (GeV)	$m(1^+)$ (GeV)
$\bar{d}c$	1.87	2.01	2.47	2.42
$\bar{s}c$	1.97	2.11	2.60	2.53
$\bar{u}b$	5.27	5.32	5.78	5.71
$\bar{s}b$	5.38	5.43	5.89	5.82
$\bar{c}b$	6.30	6.34	6.80	6.73

Table 16. Values of decay constants used in the numerical estimates

Weak current	Particle	f_M (MeV)	Weak current	Particle	F_V (MeV)
$\bar{u}d$	π^-	133	$\bar{u}d$	ρ^-	221
$\bar{d}s$	$\bar{K}^0$	162	$\bar{d}s$	$\bar{K}^{*0}$	221
$\bar{d}d$	η	68	$\bar{d}d$	ω	156
$\bar{s}s$	η	−92	$\bar{s}s$	ϕ	233
$\bar{d}d$	η'	65	$\bar{c}c$	J/Ψ	382
$\bar{s}s$	η'	96	$\bar{u}d$	A_1^-	221
$\bar{u}c$	D^0	162	$\bar{u}c$	D^{*0}	221
$\bar{s}c$	D_s^+	162	$\bar{s}c$	D_s^{*+}	221

The vector couplings are defined according to $\langle 0|J_\mu|V\rangle=\varepsilon_\mu F_V m_V$
We set $f_D=f_K$ and $F_{K^*}=F_{A_1}=F_{D^*}=F_{\rho^-}$

References

1. DELCO Collab. W. Bacino et al.: Phys. Rev. Lett. **43**, 1073 (1979); S. Stone, in: Proceedings of the 1983 International Symposium on Lepton and Photon Interactions at High Energies,

Ithaca, N.Y., eds. D.G. Cassel, D.L. Kreinick, p. 203, Cornell University 1983; H. Schröder, in: Hadron Spectroscopy – 1985 –, AIP Conf. Proc. 132: the Intern. Conf. on Hadron Spectroscopy, College Park Maryland, ed. S. Oneda, p. 368, New York: AIP 1985
2. G. Altarelli et al.: Nucl. Phys. **B208**, 365 (1982)
3. M. Wirbel, B. Stech, M. Bauer: Z. Phys. C – Particles and Fields **29**, 637 (1985); M. Wirbel in: Proceedings of the International Symposium on Production and Decay of Heavy Hadrons, Heidelberg 1986, K.R. Schubert, R. Waldi eds., p. 165, DESY
4. J.G. Körner in: Proceedings of the International Symposium on Production and Decay of Heavy Hadrons, Heidelberg 1986, K.R. Schubert, R. Waldi eds., p. 279, DESY; see also previous work by A. Ali, J.G. Körner, G. Kramer, J. Willrodt, Z. Phys. C – Particles and Fields **1**, 269 (1979)
5. B. Grinstein, M.B. Wise, N. Isgur: Phys. Rev. Lett. **56**, 298 (1986); CALT-68-1311 (1986); S. Nussinov, W. Wetzel: Cornell University Preprint CLNS 86/731 (1986)
6. S.L. Glashow, J. Iliopoulos, L. Maiani: Phys. Rev. **D2**, 1285 (1970); M.K. Gaillard, B.W. Lee, J.L. Rosner: Rev. Mod. Phys. **47**, 277 (1975); J. Ellis, M.K. Gaillard, D.V. Nanapoulos: Nucl. Phys. **B100**, 313 (1985)
7. For a complete list of references see: B.Yu. Blok, M.A. Shifman: preprint ITEP-9, Theoretical and Experimental Physics Moscow (1986)
8. M. Bauer, B. Stech: Phys. Lett. **152B**, 380 (1985); B. Stech: Proc. of the 5th Moriond Workshop on Flavour Mixing and CP Violation, 151, 1985; B. Stech in: Proc. of the Leptonic Session of the XXIst Rencontre de Moriond, Les Arcs 1986, Tran Thanh Van, (ed.). Vol. 1, Progess in Elektroweak Interactions, p. 335, Editions Frontiéres
9. Mark III Collab., R. Schindler: Presented at the Leipzig Conf. (1984); SLAC-PUB-3799 (1985); D.M. Coffmann in: Proc. of the Leptonic Session of the XXIst Rencontre de Moriond, Les Arcs 1986, Tran Thanh Van, (ed.). Vol. 1, Progess in Elektroweak Interactions, p. 271, Editions Frontiéres; D. Hitlin in: Proceedings of the International Symposium on Production and Decay of Heavy Hadrons, Heidelberg 1986, K.R. Schubert, R. Waldi (eds.), p. 105, Desy
10. I.I. Bigi, A.I. Sanda: Nucl. Phys. **B281**, 41 (1987)
11. L.L. Chau: Phys. Rep. **95**, 1 (1983)
12. For a review and many further references see e.g. R. Rückl: Weak Decays of Heavy Flavours, Habilitationsschrift Universität München, CERN print (1983)
13. M.K. Gaillard, B.W. Lee.: Phys. Rev. Lett. **33**, 108 (1974); G. Altarelli, L. Maiani: Phys. Lett. **52B**, 351 (1974); G. Altarelli, G. Corci, G. Martinelli, R. Petrarca: Nucl. Phys. **B187**, 461 (1981); W. Bernreuther: Z. Phys. C – Particles and Fields **29**, 245 (1985); Ann. Phys. (N.Y.) **151**, 127 (1983)
14. M.A. Shifman, A.I. Vainshtein, V.I. Zakharov: Nucl. Phys. **B120**, 315 (1977)
15. F. Gilman, M.B. Wise: Phys. Rev. **D20**, 2392 (1979)
16. D. Fakirov, B. Stech: Nucl. Phys. **B133**, 315 (1978); N. Cabibbo, L. Maiani: Phys. Lett. **73B**, 418 (1978)
17. T.D. Lee, in: Theory and phenomenology of particle physics. Erice 1968, ed. A. Zichichi, p. 262, New York: Academic Press 1969
18. R.P. Feynman, in: Symmetries in elementary particle physics, ed. A. Zichichi, p. 167, New York: Academic Press 1965; O. Haan, B. Stech: Nucl. Phys. **B22**, 448 (1970)
19. A.J. Buras, J.-M. Gérard, R. Rückl.: Nucl. Phys. **B268**, 16 (1986)
20. N. Desphande, M. Gronau, D. Sutherland: Phys. Lett. **90B**, 431 (1980)
21. Y. Koide, Phys. Rev. **D19**, 2631 (1979)
22. H.J. Lipkin: Phys. Lett. **90B**, 710 (1980)
23. V. Lüth: Presented at the Physics in Collision V Conference Autun, France 1985; preprint CERN-EP/185-142, 1985
24. M. Einhorn, C. Quigg: Phys. Rev. **D12**, 2015 (1975)
25. B. Guberina, R.D. Peccei, R. Rückl: Phys. Lett. **89B**, 111 (1979)
26. ARGUS Collab. H. Albrecht et al.: Phys. Lett. **158B**, 525 (1985); CLEO Collab. C. Bebek et al.: Phys. Rev. Lett. **56**, 1893 (1986); MARK III Collab. R.M. Baltrusaitis et al.: SLAC-PUB-3858 to appear in Phys. Rev. Lett.
27. J.F. Donoghue: Phys. Rev. **D33**, 1516 (1986)
28. M. Bander, D. Silvermann, A. Soni: Phys. Rev. Lett. **44**, 7, 962 (E) (1980); W. Bernreuther, O. Nachtmann, B. Stech: Z. Phys. C – Particles and Fields **4**, 257 (1980); H. Fritzsch, P. Minkowski: Phys. Lett. **90B**, 455 (1980)
29. I.I. Bigi, M. Fukugita: Phys. Lett. **91B**, 121 (1980)
30. L.-L. Chau, H.-Y. Cheng: Phys. Rev. Lett. **56**, 1655 (1986)
31. U. Baur, A.J. Buras, J.-M. Gérard, R. Rückl: Phys. Lett. **B175**, 377 (1986); A.N. Kamal, Phys. Rev. **D33**, 1344 (1986)
32. M. Lusignoli, A. Pugliese: preprint 515, 10 Luglio 1986 Roma
33. T. Armstrong et al.: Nucl. Phys. **B221**, 1 (1983)
34. G. Bellini et al.: Phys. Rev. Lett. **48**, 1697 (1982)
35. ARGUS Collab. H. Albrecht et al.: Phys. Lett. **B179**, 398 (1986)
36. Particle Data Group: Phys. Lett. **170B**, 1 (1986)
37. X.Y. Pham.: preprint PARIS LPTHE 86/10 February 1986; A.I. Sanda: Phys. Rev. **D22**, 2814 (1980)
38. B.Yu. Blok, M.A. Shifman: preprint ITEP-37, Theoretical and Experimental Physics Moscow (1986)
39. ARGUS Collab. K.R. Schubert: Presented at the XXIIIrd International Conference on High Energy Physics, Berkely (1986); CLEO Collab. M.G.D. Gilchriese: Presented at the XXIIIrd International Conference on High Energy Physics, Berkely (1986)
40. H. Fritzsch: Phys. Lett. **73B**, 317 (1978)
41. B. Stech: Phys. Lett. **130B**, 189 (1983); B. Stech, in: Flavour mixing in weak interaction, Ett. Majorana, Int. Series Physical Sciences Vol. 20, p. 735–759, ed. L.L. Chau New York: Plenum Press 1984
42. M. Gronau, R. Johnson, J. Schechter: Phys. Rev. Lett. **54**, 2176 (1986)
43. B. Guberina, R.D. Peccei, R. Rückl: Phys. Lett. **90B**, 169 (1980)
44. A. Le Yaouanc in: Proceedings of the International Symposium on Production and Decay of Heavy Hadrons, Heidelberg 1986, K.R. Schubert, R. Waldi (eds.), p. 285, Desy; M.B. Gavela et al.: Phys. Lett. **154B**, 425 (1985)